한국해안·해양공학회 학술발표논문집 (2008)
2008년 9월 25일-9월 26일
제17권, pp. 204-207

Numerical Simulation of Shallow-water Waves Propagating over Arbitrary Bottom Topography using Boussinesq Equations

Boussinesq방정식을 이용한 임의바닥지형을 진행하는 천수역파의 수치모사

Rae Hyoung Yuck[1], Byoung Won Park[1], **Hang Shoon Choi[2]**
육래형[1], 박병원[1], 최항순[2]

1. INTRODUCTION

Wave effects must be taken carefully into account for the design of coastal structures such as breakwater, harbor, and moored-floater. Normally a number of possible wave conditions are examined in order to determine the design criteria. The wave conditions can be generated by a suitable mathematical model with help of numerical methods, which must be able to describe wave deformations accurately in terms of shoaling, refraction, diffraction and reflection of waves propagating from deep water to shallow water.

Boussinesq models are well known as the most accurate method for dealing with the propagation of non-linear shallow water waves near coastal regions. Boussinesq (1872) derived the equation by eliminating the vertical dependency and assuming $O(\mu^2)=O(\varepsilon)<1$, where $\mu=k_0h_0$, $\varepsilon=a_0/h_0$. k_0, a_0 and h_0 are the typical wave number, amplitude and the water depth in this order at a far upstream reference location. For waves propagating in intermediate or deep water, the modified Boussinesq equations with improved dispersion characteristics have been suggested. Madsen et al (1992) included higher-order terms with adjustable coefficients in the standard Boussinesq equation for even and variable bottoms. Agnon et al. (1999) formulated exactly the boundary conditions at the free surface and the bottom in an approximate solution of the Laplace equation, which is expressed by truncated series expansions. As a result, this formulation gives an accurate nonlinear dispersion relation up to $kh=6$.

Above methods, however, do not provide an accurate vertical distribution of the velocity field. Madsen et al. (2002) suggested a new type of non-linear wave equations retaining the vertical velocity as an unknown. In this method, the Laplace solution is expanded from an arbitrary z-level rather than the still-water, which is quite different from the conventional Boussinesq equations. His fifth-order model can describe highly non-linear waves accurately up to $kh=25$ from the viewpoint of dispersion property, and up to $kh=12$ from the viewpoint of vertical velocity profile. Based on this approach, numerical simulations are carried out for waters of slowly-varying bathymetry in this work. Hereby numerical methods applicable for shoaling, refraction and also irregular wave propagation are rigorously implemented. The results thus obtained for wave profile, vertical structure of velocities and irregular wave propagation are to be used as input data for the motion analysis of floaters in shallow waters.

2. BOUSSINESQ FORMULATION

It is assumed that the fluid is incompressible and inviscid with a free surface. A Cartesian coordinate system is introduced with x- and y-axis located on the still-water plane. Z-axis is pointed vertically upward. The kinematic and dynamic free-surface conditions are

1 서울대학교 조선해양공학과
2 발표자: 서울대학교 조선해양공학과 교수

$$\eta_t - \tilde{w} + \nabla\eta \cdot \tilde{\mathbf{V}} = 0 \tag{1}$$

$$\tilde{\mathbf{V}}_t + g\nabla\eta + \nabla[\frac{\tilde{\mathbf{V}}\cdot\tilde{\mathbf{V}}}{2} + \frac{\tilde{w}}{2}(1-\nabla\eta\cdot\nabla\eta)] = 0, \tag{2}$$

where $\tilde{\mathbf{V}} = \tilde{\mathbf{u}} + \tilde{w}\nabla\eta$ (3)

Here $\tilde{\mathbf{u}} = <\tilde{u}, \tilde{v}>$ and $\tilde{w}$ are the horizontal and vertical velocities at the free-surface, respectively. g denotes the gravitational acceleration and $\nabla \equiv (\partial/\partial x, \partial/\partial y)$ the horizontal gradient operator. Accordingly, the kinematic bottom condition is expressed by

$$w_b + \nabla h \cdot u_b = 0. \tag{4}$$

The equations given in (1)-(3) represent a fully non-linear time-stepping problem. The vertical and horizontal velocities at an arbitrary z-level are related with those at the reference z-level by trigonometric functions, which satisfy the Laplace equation in the interior fluid domain. The accuracy of the trigonometric funtionals is enhanced greatly by applying the Padé expansions (Padé, 1892). Finally the velocities are expressed by

$$\begin{aligned} u(x,y,z,t) = {} & (1-\alpha_2\nabla^2+\alpha_4\nabla^4)\hat{\mathbf{u}}^*(x,y,t) \\ & +((z-\hat{z})\nabla-\beta_3\nabla^3+\beta_5\nabla^5)\hat{w}^*(x,y,t)+\Lambda_u\nabla\tilde{z} \end{aligned} \tag{5}$$

$$\begin{aligned} w(x,y,z,t) = {} & (1-\alpha_2\nabla^2+\alpha_4\nabla^4)\hat{w}^*(x,y,t) \\ & -((z-\hat{z})\nabla-\beta_3\nabla^3+\beta_5\nabla^5)\hat{\mathbf{u}}^*(x,y,t)+\Lambda_w\nabla\tilde{z} \end{aligned} \tag{6}$$

, where

$$\alpha_2 = \frac{(z-\hat{z})^2}{2} - \frac{\hat{z}}{18},\quad \alpha_4 = \frac{(z-\hat{z})^4}{24} - \frac{\hat{z}^2(z-\hat{z})^2}{36} + \frac{\hat{z}^4}{504},$$
$$\beta_3 = \frac{(z-\hat{z})^3}{6} - \frac{\hat{z}^2(z-\hat{z})}{18},\quad \beta_5 = \frac{(z-\hat{z})^5}{120} - \frac{\hat{z}^2(z-\hat{z})^3}{108} + \frac{\hat{z}^4(z-\hat{z})}{504}. \tag{7}$$

In equations (5) and (6), the quantities $\hat{\mathbf{u}}^*$ and $\hat{w}^*$ are the so-called utility variables which are introduced for the approximate solution of the Laplace equation. It is known that an optimal velocity distribution can be obtained near $\hat{z} = -h/2$ (Madsen et al, 2002). This choice is kept also in this paper. With this Boussinesq formulation, the velocity components at the free-surface and the bottom can be obtained by substituting $z = \eta$ and $z = -h$,respectively. By inserting equations (5) and (6) into the bottom boundary condition, equation(4), we have a relation for the utility velocities $\hat{\mathbf{u}}^*$ and $\hat{w}^*$.

$$\begin{aligned} & (1-\frac{4}{9}\gamma^2\nabla^2+\frac{1}{63}\gamma^3\nabla^3)\hat{w}^* + (\gamma\nabla-\frac{1}{9}\gamma^3\nabla^3+\frac{1}{945}\gamma^5\nabla^5)\hat{\mathbf{u}}^* \\ & +\nabla h\cdot(1-c_2\gamma^2\nabla^2+c_4\gamma^4\nabla^4)\hat{\mathbf{u}}^* - \nabla h\cdot(\gamma\nabla-s_3\gamma^3\nabla^3+s_5\gamma^5\nabla^5)\hat{w}^* = 0, \end{aligned} \tag{8}$$

where $\gamma = (h+\hat{z})$.

Here, the coefficients of the bottom slope terms are modified in order to satisfy the linear shoaling gradient numerically. The optimized coefficients are found to be $c_2 = 0.357739$, $c_4 = 0.00663819$, $s_3 = 0.0753019$, $s_5 = -6.31532\times10^{-5}$ for $kh \le 30$ (Madsen et al., 2002). Combining $\tilde{\mathbf{V}}$ in equation (3) and the bottom boundary condition (8), the following linear system is established.

$$\begin{bmatrix} A_1-\eta_x B_{11} & -\eta_x B_{12} & B_{11}+\eta_x A_1 \\ -\eta_y B_{11} & A_1-\eta_y B_{12} & B_{12}+\eta_y A_1 \\ A_{01}+h_x I_1 & A_{02}+h_y I_1 & B_0-h_x I_{13}-h_y I_{23} \end{bmatrix} \begin{bmatrix} \hat{u}^* \\ \hat{v}^* \\ \hat{w}^* \end{bmatrix} = \begin{bmatrix} \tilde{u} \\ \tilde{v} \\ 0 \end{bmatrix} \tag{9}$$

Here, the subscripts x and y denote the partial differentiation with respect to each variable. This system has a number of operators which contain up to either fourth-order or fifth-order mixed derivatives related with equations (5) and (6). The utility velocity components $\hat{\mathbf{u}}^*$ and $\hat{w}^*$ can be solved from equation (9) in terms of $\tilde{\mathbf{u}}$ and η. After having solved the utility variables, the vertical velocity at the free-surface, $\tilde{w}$, can be computed from Boussinesq formulation (6), i.e.

$$\tilde{w} = A_1\hat{w}^* - B_{11}\hat{u}^* - B_{12}\hat{v}^*, \tag{10}$$

which is used to close the governing equation. Finally the problem turns out to be a time-stepping problem for the non-linear free-surface boundary conditions, equations (1) and (2).

3. MODEL VERIFICATION

3.1 Linear Wave Shoaling

The linear shoaling equation is defined by (Madsen and Sorensen, 1992).

$$\frac{A_x}{A} = -\alpha\frac{h_x}{h} \tag{11}$$

The shoaling gradient, α, can be derived by using energy flux conservation combined with Stokes linear theory,

$$\alpha_s = \frac{G(1+0.5G(1-\cosh 2kh))}{(1+G)^2}, \qquad (12)$$

where $G \equiv \frac{2kh}{\sinh 2kh}$.

To exemplify the present method, the following test case is considered herein. At the seaward boundary, the water depth is 13m. The bottom is flat for the first 10m from the seaward boundary, while it has a constant slope of 1/50 from 10m to 600m from the boundary. From 600m to 650m, the bottom is flat again with a water depth of 1.2m. All non-linear terms are switched off in this particular simulation, the grid size and time step are chosen to be 1.0m and 0.08s, respectively.

The computed surface elevation is shown in Fig.1, while Fig.2 shows the comparison between the computed maximum elevation and the shoaling curve obtained from equation (12) with the exact shoaling gradient (11). The agreement is quite well over all locations. Based on this simulation, it is concluded that the accuracy of the present numerical model is acceptable for mild wave shoaling.

3.2 Nonlinear Wave Shoaling

Whalin's experiment (1971) is often cited in literature to validate numerical wave models involving both the refraction and the shoaling. The topography is given by equation (13) and shown in Fig.3, i.e. the shoaling region looks like a concave lens.

$$h(x,y) = \begin{cases} 0.4572 & \text{if } 0 \le x \le 10.67 - G \\ 0.4572 + \frac{1}{25}(10.67 - G - x) & \text{if } 10.67 - G \le x \le 18.29 - G \\ 0.1524 & \text{otherwise} \end{cases} \qquad (13)$$

, where $G(y) = \sqrt{y(6.096 - y)}$.

The gradient of h is calculated analytically when building the bottom boundary condition (4). Because the bathymetry is symmetrical about centerline $y = 3.048m$, only the half of the domain is considered. For waves of T=1s, it corresponds to kh=1.913 and ka=0.0816. The mesh with 40 nodes per wave length is used and the time step is fixed to be $\Delta t = T/40$. Almost identical results for the 1^{st} order harmonic are obtained as shown in Fig.4. These are the relative amplitudes of harmonics along the center line at y=3.048m.

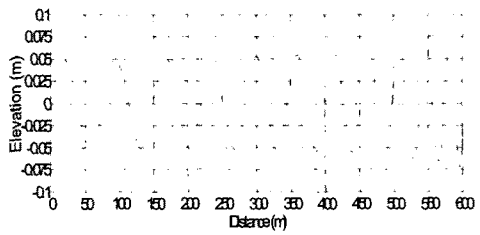

Fig. 1. Calculated Free-surface Elevation

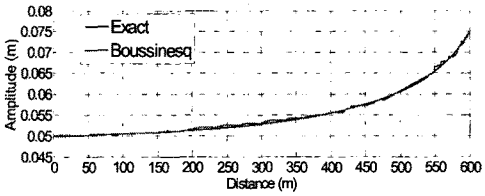

Fig. 2. Comparison of Calculated Maximum Elevation with Exact Linear Solution

Comparisons between the numerical and experimental results are quite good. The numerical reflection is not observed even for second harmonics because we use 40 nodes for the primary wave, which correspond to 20 nodes for the second harmonic waves. The wave focusing can be seen in Fig.5, which implies the capability of the Boussinesq formulation and the present method.

3.3 Irregular Wave Simulation

Irregular waves in a water of constant depth are simulated to investigate the generation and absorption characteristics of irregular waves in shallow water. It is to note that the peak frequency of the simulated wave spectrum is in the shallow water region ($kh \le 1.0$). The irregular waves are imposed at the inlet boundary using JONSWAP spectrum which has the peak period of 12s and the significant wave height of 3m. Fig. 6 shows the generated wave spectrum. Two spectra match each other quite well with relative error less than 1% in the sense of the total energy. Based on this result, it may be concluded that there is not significant numerical dissipation in the interior domain and the absorption layer works well for waves of practically all frequencies.

5. CONCLUSION

A high-order Boussinesq equation based on the Padé expansion is modeled to simulate the fully non-linear and highly dispersive waves.

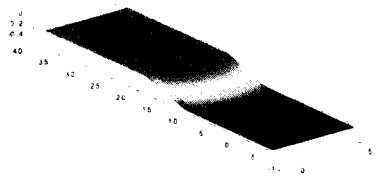

Fig. 3. Bottom Topology for Nonlinear Wave Shoaling

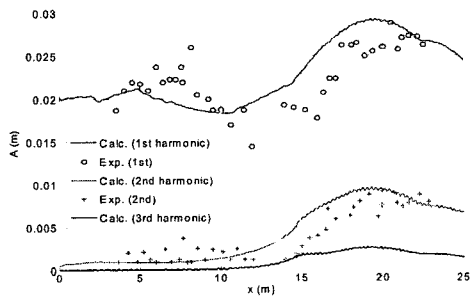

Fig. 4. Computed and Measured Harmonic Amplitudes for Whalin's Experiment

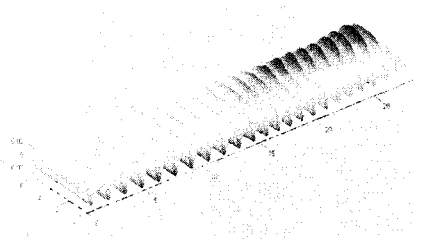

Fig. 5. Snap Shot of Simulated Nonlinear Surface Elevation

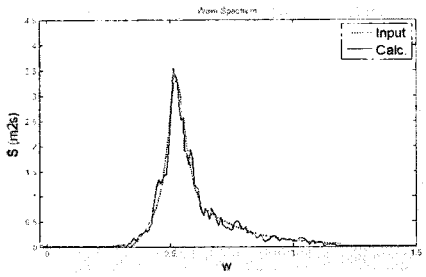

Fig. 6. Comparison Between Input Wave Spectrum and Generated Wave Spectrum

The formulation is expressed by the velocity field in terms of finite series expansions of velocity components at an arbitrary z-level. This method makes possible to extend the applicability of the Boussinesq equations to the deeper water region and it turns out for the dispersion relation to be accurate as high as $kh = 25$, while for the vertical structure of the velocity field as high as $kh = 12$.

The present numerical result compares quite well with the corresponding experiment (or exact solution) for several cases considered herein. The simulation of linear and nonlinear shoaling shows the accurate shoaling characteristics. The simulation for the irregular waves in shallow water regions shows good correspondence of the total energy between the input and generated wave spectrum.

REFERENCES

Agnon, Y, Madsen,PA.,Schaffer,HA(1999). A new approach to high order Boussinesq models. J. of Fluid Mechanics, 399, 319-333.

Boussinesq, MJ (1872). Théorie des ondes et des ramous qui se propagent le long d'nn canal rectagulaire horizontal, en communiquant au liquid contenu dans ce canal des vitesses sensiblement pareilles de la surface au fond. J. Math. Pures Appliq., 17, 55-108.

Fuhrman, DR, Bingham, HB (2004). Numerical solutions of fully non-linear and highly dispersive Boussinesq equations in two horizontal dimensions. J. of Number. Meth. Fluids, 44, 321-255.

Madsen, PA, Bingham, HB, Liu, H (2002). A new Boussinesq method for fully nonlinear waves from shallow to deep water. J. of Fluid Mechanics, 462, 1-30.

Madsen, PA, Bingham, HB, Shaffer, HA (2003). Boussinesq formulations for fully non-linear and extremely dispersive water waves. Philosophical Transactions of the Royal Society of London Series A, 459, 1075-1104.

Madsen, PA., Sorensen OR (1992). A new form of the Boussinesq equations with improved linear dispersion characteristics. Part2. A slowly-varying bathymetry. J. Of coastal Engineering, 18, 183-204.

Padé, H (1892). Sur la representation approchee d'une function par des fractions rationelle. Annals d' ecoles, 9.

Peregrine, DH (1967). Long waves on a beach. J. of Fluid Mech., 27, 815-827.

Whalin, RW (1971). The limit of applicability of linear wave refraction theory in convergence zone. Res. Rep. H-71, U.S. Army Corp. of Engineers.